

MASSACHUSETTS INSTITUTE OF TECHNOLOGY
ARTIFICIAL INTELLIGENCE LABORATORY

WORKING PAPER 169

May 1978

LOOKING IN THE SHADOWS

Robert J. Woodham

Berthold K. P. Horn

ABSTRACT

The registration of an image with a model of the surface being imaged is an important prerequisite to many image understanding tasks. Once registration is achieved, new image analysis techniques can be explored. One approach is to compare the real image with an image synthesized from the surface model. But, accurate comparison requires an accurate synthetic image.

More realistic synthetic images can be obtained once shadow information is included. Accurate shadow regions can be determined when a hidden-surface algorithm is applied to the surface model in order to calculate which surface elements can be seen from the light source. We illustrate this technique using LANDSAT imagery registered with digital terrain models. Once shadow information is included, the effect of sky illumination and atmospheric haze can be measured.

A. I. Laboratory Working Papers are produced for internal circulation, and may contain information that is, for example, too preliminary, or too detailed for formal publication. Although some will be given a limited external distribution, it is not intended that they should be considered papers to which reference can be made in the literature.

This report describes research done at the Artificial Intelligence Laboratory of the Massachusetts Institute of Technology. Support for the laboratory's artificial intelligence research is provided in part by the Advanced Research Projects Agency of the Department of Defense under Office of Naval Research contract N00014-75-C-0643.

© MASSACHUSETTS INSTITUTE OF TECHNOLOGY 1978

1. Motivation

Interesting and useful new image analysis methods can be developed once registered image intensity and surface slope information is available. The accurate alignment of images with surface models is an important prerequisite to many image understanding tasks. Synthesized images have been shown to be a useful intermediary in the automatic registration of real images with surface models[1]. Simple, idealized models of reflectance are sufficient to generate the synthetic images required for alignment. Because registration using synthetic images is an area-based computation, high accuracy is attainable despite many factors which can contribute to local differences between the real and synthetic images.

Once registration has been achieved, it becomes possible to consider exploiting these local differences. Automatic classification of terrain from LANDSAT imagery, for example, can benefit from a point-by-point comparison of synthetic and real image intensity. Roughly speaking, intensity fluctuations in satellite imagery combine effects due to variations in surface slope and effects due to variations in ground cover. Note, however, that all LANDSAT images are taken at about 9:30 AM local solar time. With the sun low in the sky, intensity fluctuations due to variations in surface slope often swamp intensity fluctuations due to variations in ground cover. On the other hand, if the synthetic image accurately captures fluctuations due to surface slope, then remaining differences are caused by variations in ground cover.

A more accurate synthetic image can be obtained once shadow information is included. Looking in regions shadowed from the sun allows one to estimate the effect of sky illumination and atmospheric haze. Including these effects in the synthetic image is necessary to relate remaining differences between the real and synthetic images to ground cover.

Accurate shadow regions can be determined when a hidden-surface algorithm is applied to the surface model in order to calculate which surface elements can be seen from the source. We illustrate this technique using LANDSAT imagery registered to digital terrain models.

2. Digital Terrain Models

Recent work on computer-based methods for cartography and machines that analyze stereo aerial photography has led to the development of digital terrain models[2]. These models are usually in the form of an array of terrain elevations on a regular grid. Grid points can be actual geographic coordinates or coordinates corresponding to a given map projection.

3. The Reflectance Map

Work on image understanding has led to a need to model the image-forming process. One aspect of this concerns the geometry of image projection. Less well understood is the radiometry of image formation. Determining the intensity values recorded in an image requires a model of the way surfaces reflect light.

The reflectance map is a convenient way to explicitly model surface reflection. For a particular surface material and a particular placement of light sources, surface reflectance can be plotted as a function of surface gradient. The result is called a *reflectance map* and is usually presented as a contour map of constant reflectance in gradient space[3].

One use of the reflectance map is the determination of surface shape from image intensity[4,5]. Here, however, it will be employed only in order to generate synthetic images from digital terrain models.

4. Surface Gradient

Two degrees of freedom are required to specify a surface gradient. One way to express the gradient is to specify the surface slope along two mutually perpendicular directions. Suppose terrain elevation, z , is given as a function $z = f(x,y)$ of two spatial coordinates x and y . Define the two components, p and q , of the gradient as the partial derivatives of $z = f(x,y)$ with respect to x and y respectively. If a Cartesian coordinate system is erected with the x -axis pointing east, the y -axis north and the z -axis up, then, p is the surface slope in the west-to-east direction and q is the surface slope in the south-to-north direction.

One can estimate p and q from the digital terrain model using first differences. More sophisticated interpolation schemes are possible, but were not found necessary.

5. Satellite Ephemeris/Attitude

In order to generate the synthetic image, we assume a distant spacecraft looking vertically downward with a narrow angle of view. The image y -axis is assumed to point north and the x -axis east. With this imaging geometry, a simple orthographic projection is appropriate to relate points in the synthetic image to points in the digital terrain model. Because of the happy alignment of the z -axis, in the digital terrain model, and the satellite viewing direction, there is no hidden-surface elimination problem from the viewpoint of the satellite. Each surface element in the digital terrain model generates a picture element in the synthetic image.

In reality, the relationship between LANDSAT image coordinates and ground coordinates is more complicated[6]. Here, we assume that the real satellite imagery has already been registered to the digital terrain model so that an idealized model of satellite imaging geometry suffices.

6. The Position of the Sun

In order to determine the reflectance map, it is necessary to know the location of the light sources. For LANDSAT imagery, the primary source we wish to consider is the sun. The position of the sun is easily determined using tables intended for celestial navigation[7,8,9] or by straightforward computations[10,11,12,13]. In either case, given a date, time and position on the earth's surface, the elevation (ϕ) and azimuth (θ) of the sun can be found. Here, elevation is the angle between the sun and the horizon and azimuth is measured clockwise from north (see figure 1).

The position of the sun can also be represented using gradient coordinates p and q . Let the vector pointing at the sun have gradient (p_s, q_s) . Then,

$$p_s = \sin(\theta) \cot(\phi) \quad (1)$$

$$q_s = \cos(\theta) \cot(\phi) \quad (2)$$

7. Shadow Determination

In order to determine surface elements which lie in shadow, it is convenient to consider the position of the sun to be that of a viewer and then apply a hidden-surface algorithm from that viewpoint.

Erect a display coordinate system (x_s, y_s, z_s) at the sun with (x_s, y_s) the image-plane coordinates and z_s pointing in the direction of view. The transformation from earth coordinates (x, y, z) to display coordinates (x_s, y_s, z_s) can be developed as combination of a rotation and translation[14]. Here, we will determine the transformation from earth coordinates (x, y, z) to image points (x_s, y_s) directly. To do this, we need to develop expressions for x_s and y_s in terms of x , y and z and sun parameters ϕ and θ .

First, consider the effect of the azimuth θ . If $\theta = \pi$ radians, then the y_s -axis would point directly north. In general, the y_s -axis is oriented $(\pi - \theta)$ degrees measured clockwise from north. Thus, the earth (x,y) coordinate axes can be aligned with display coordinate axes (x_s,y_s) by rotating the earth coordinates through an angle $(\pi - \theta)$.

Next, consider the effect of the elevation ϕ . The elevation ϕ causes foreshortening along the Y_s -axis. The z earth coordinate is foreshortened by $\cos(\phi)$ while the component of (x,y) along the Y_s -axis is foreshortened by $\sin(\phi)$. The component of (x,y) along the X_s -axis is unchanged.

The overall transformation from digital terrain point $z = f(x,y)$ to display point (x_s,y_s) is given by:

$$x_s = x \cos(\pi - \theta) + y \sin(\pi - \theta) \tag{3}$$

$$y_s = z \cos(\phi) + \sin(\phi)[y \cos(\pi - \theta) - x \sin(\pi - \theta)] \tag{4}$$

One way to do hidden-surface elimination would be to explicitly compute the corresponding depth value z_s associated with each surface point (x,y,z) [15]. Then, the decision whether or not a point (x_s,y_s,z_s) is in view would depend upon whether or not the depth value z_s is less than the depth value associated with other points which project to (x_s,y_s) .

If, on the other hand, the surface is known explicitly as a function $z = f(x,y)$, then a uniform profile expansion can be used to eliminate the need to explicitly calculate depth. By systematically expanding surface profiles away from the viewer, the decision to display at a particular image point (x_s,y_s) reduces to a simple comparison of the y_s coordinate against the largest y_s coordinate so far displayed at the particular x_s [16].

Depth information is implicitly represented as a one-dimensional array holding the largest y_s coordinate displayed for each x_s . The systematic profile expansion insures that a displayed image point (x_s,y_s) corresponds to a visible surface point (x,y,z) . For display purposes, points not in view are simply

ignored. For shadow determination, points not seen by the light source correspond to shadowed regions of the surface.

8. Modeling Surface Reflectance

Surface reflectance can be expressed as a function of the incident angle i , the emittance angle e and the phase angle g (see figure 2). One simple, idealized reflectance function for surface material is given by:

$$\phi_1(i, e, g) = \rho \cos(i) \quad (5)$$

This reflectance function models a surface which appears equally bright from all viewing directions. Here, ρ is an "albedo" factor and the cosine of the incident angle accounts for the foreshortening of the surface element as seen by the source.

Another idealized reflectance function is given by:

$$\phi_2(i, e, g) = \rho \cos(i) / \cos(e)$$

This reflectance function models a surface which reflects equal amounts of light in all directions. Here, the cosine of the emittance angle accounts for the foreshortening of the surface element as seen by the viewer.

Both reflectance functions have been used to generate synthetic images for the automatic registration of LANDSAT images with digital terrain models[1]. More sophisticated models are not required for the area-based computations used to achieve precise alignment. High accuracy is attainable despite many factors which contribute to local differences between the real and synthetic image.

Once registration is achieved, one would like to exploit these local differences. But, exploiting local differences requires a more realistic synthetic image. Additional realism can be achieved in synthesized satellite images if effects due to sky illumination and haze are included.

The following equation attempts to model these additional effects. Synthetic image intensity is given by $I'(x,y)$ where:

$$I'(x,y) = a \phi(i,e,g) + b z + c \quad (7)$$

and

$$\phi(i,e,g) = \begin{cases} \cos(i) & \text{if } (x,y) \text{ illuminated} \\ 0 & \text{if } (x,y) \text{ lies in shadow} \end{cases}$$

As in (5) above, $\phi(i,e,g)$ models a surface which, appears equally bright from all viewing directions. Note, however, that cast shadows are now included. Here, "a" is the albedo factor. To a first approximation, sky illumination is considered a constant. At the same time, attenuation of reflected energy occurs due to atmospheric haze. This attenuation is a function of elevation. Here, "b" and "c" model sky illumination and atmospheric haze as a first-order function of terrain elevation.

9. Estimating Parameters b and c

Parameters b and c can be estimated by looking in regions where $\phi(i,e,g)$ is zero in (7) above (i.e., by looking in the shadows). This is illustrated in the following example.

10. An Example

Digital terrain data for the example used here was entered into a computer after manual interpolation from a contour map and has been used previously in work on automatic hill-shading[17] and automatic image registration[1]. It consists of an array of 175 x 240 elevations on a 100-meter grid corresponding to a 17.5 x 24.0 km region of Switzerland lying between $7^{\circ} 1'$ east to $7^{\circ} 15'$ east and $46^{\circ} 8.5'$ north to $46^{\circ} 21.5'$ north. The vertical quantization is 10 meters. Elevations range from 410 meters in the Rhone valley to 3210 meters on the Sommet des Diablerets. The topographic maps used in the generation of the data were "Les Diablerets" (No. 1285) and "Dent de Morcles"

(No. 1305), both on a 1:25,000 scale[18]. Extensive data editing was necessary to remove entry errors. Some minor distortions of elevations may have resulted.

The images used for this paper's illustrations are a portion of LANDSAT image 1078-09555 acquired about 9:55 GMT 1972/Oct/9. Data was obtained directly from the computer compatible tape supplied by EROS[19]. Radiometric correction was applied to remove regular striping effects[20]. The image was registered to the digital terrain model using techniques described in [1].

An initial pass is required to determine which points lie in shadow. Shadow information is preserved as a one bit flag attached to each point in the digital terrain model. For a given sun position, the flag is "on" if the point lies in shadow and "off" otherwise. Two sun positions are illustrated. The first places the sun at elevation 34.2° and azimuth 154.8° , corresponding to its true position at 9:55 GMT 1972/Oct/9, while the second places it at elevation 28° and azimuth 223° , corresponding to its true position at 13:48 GMT later on the same day.

The result of shadow computation for the two sun positions is shown in figure 3. Dark points correspond to shadow points, light points correspond to points illuminated directly by the sun. As a side-effect of the shadow calculation, plots of what the terrain would look like from the point of view of the sun can also be generated. Figure 4 illustrates these.

For the sun at elevation 34.2° and azimuth 154.8° , approximately 9.7% of the terrain points lie in shadow. Figure 5 shows image intensity plotted against elevation for each of the four spectral bands recorded by LANDSAT-1. Observe that the effect of sky illumination and haze is most noticeable in band 4 (500-600 nm) and least so in band 7 (800-1100 nm). There is also a noticeable dependence of sky illumination and haze on terrain elevation.

11. References

- [1] B. K. P. Horn & B. L. Bachman, "Using Synthetic Images to Register Real Images with Surface Models", A.I. Memo 437, AI Laboratory, M.I.T., Cambridge, Mass., August 1977.
- [2] Proceedings of the *Digital Terrain Models (DTM) Symposium*, (Library of Congress 78-56346), American Society of Photogrammetry, St. Louis, Missouri, May 1978.
- [3] B. K. P. Horn, "Understanding Image Intensity", *Artificial Intelligence*, Vol. 8, pp 201-231, April 1977.
- [4] B. K. P. Horn, "Obtaining Shape from Shading Information", in P. H. Winston (ed.), *The Psychology of Computer Vision*, New York, McGraw-Hill, pp 115-155, 1975.
- [5] R. J. Woodham, "A Cooperative Algorithm for Determining Surface Orientation from a Single View", in *Proceedings of IJCAI-77*, pp 635-641, August 1977.
- [6] B. K. P. Horn & R. J. Woodham, "LANDSAT MSS Coordinate Transformations", A.I. Memo 465, AI Laboratory, M.I.T., Cambridge, Mass., February 1978.
- [7] "The Nautical Almanac for the Year 1972", U.S. Government Printing Office, Washington D.C. 20402.
- [8] "The American Ephemeris and Nautical Almanac for the Year 1972", U.S. Government Printing Office, Washington D.C. 20402.
- [9] "Explanatory Supplement to the Astronomical Ephemeris and the American Ephemeris and Nautical Almanac", Her Majesty's Stationery Office, London, England, 1961.
- [10] S. Newcomb, *A Compendium of Spherical Astronomy*, New York, McMillan & Co., 1895, 1906.
- [11] W. M. Smart, *Textbook on Spherical Astronomy*, Cambridge, Cambridge University Press, 1931, 1965.
- [12] E. W. Woolard & G. M. Clemence, *Spherical Astronomy*, Cambridge, Cambridge University Press, 1966.
- [13] B. K. P. Horn, "The Position of the Sun", Working Paper 162, AI Laboratory, M.I.T., Cambridge, Mass., March 1978.
- [14] W. M. Newman & R. F. Sproull, *Principles of Interactive Computer Graphics*, McGraw-Hill, 1973.
- [15] E. Catmull, "A Subdivision Algorithm for Computer Display of Curved Surfaces", UTEC-CSc-74-133, University of Utah, December 1974.
- [16] R. J. Woodham, "Two Simple Algorithms for Displaying Orthographic Projections of Surfaces", Working Paper 126, AI Laboratory, M.I.T., Cambridge, Mass., August 1976.

- [17] B. K. P. Horn, "Automatic Hill-Shading Using the Reflectance Map", (unpublished), 1976.
- [18] Carte Nationale de la Suisse, Swiss National Tourist Office, New York, New York.
- [19] "Computer Compatible Tape (CCT) Index", EROS Data Center, Sioux Falls, South Dakota 57198.
- [20] B. K. P. Horn & R. J. Woodham, "Destriping Satellite Images", A.I. Memo 467, AI Laboratory, M.I.T., Cambridge, Mass., March 1978.

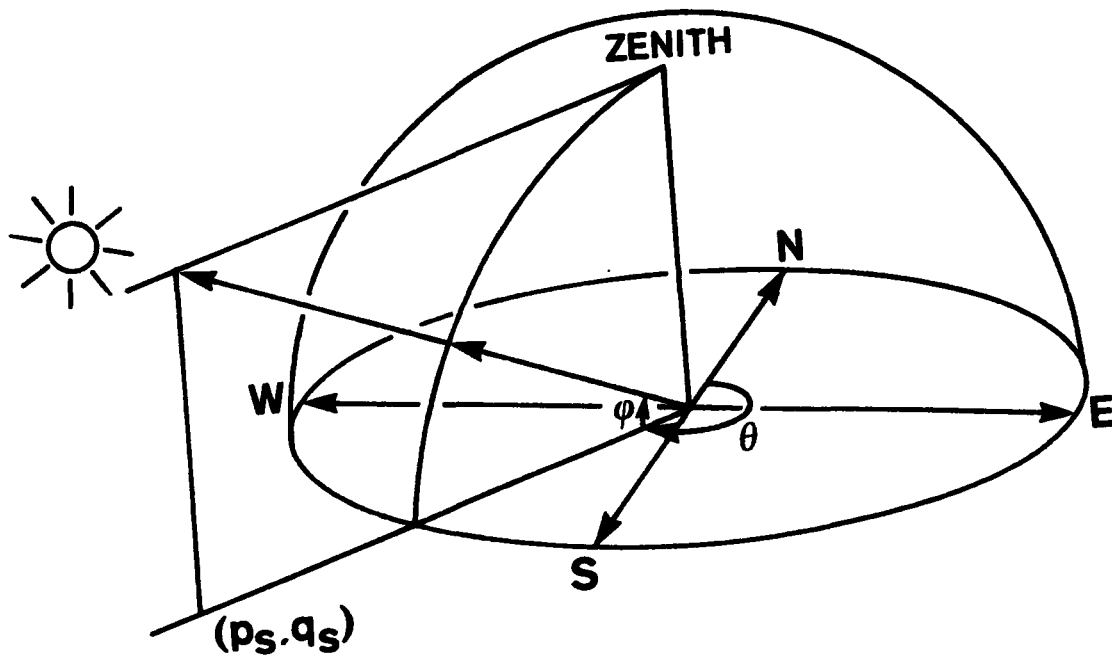


Figure 1 Defining the position of the sun in terms of the elevation angle ϕ and the azimuth angle θ .

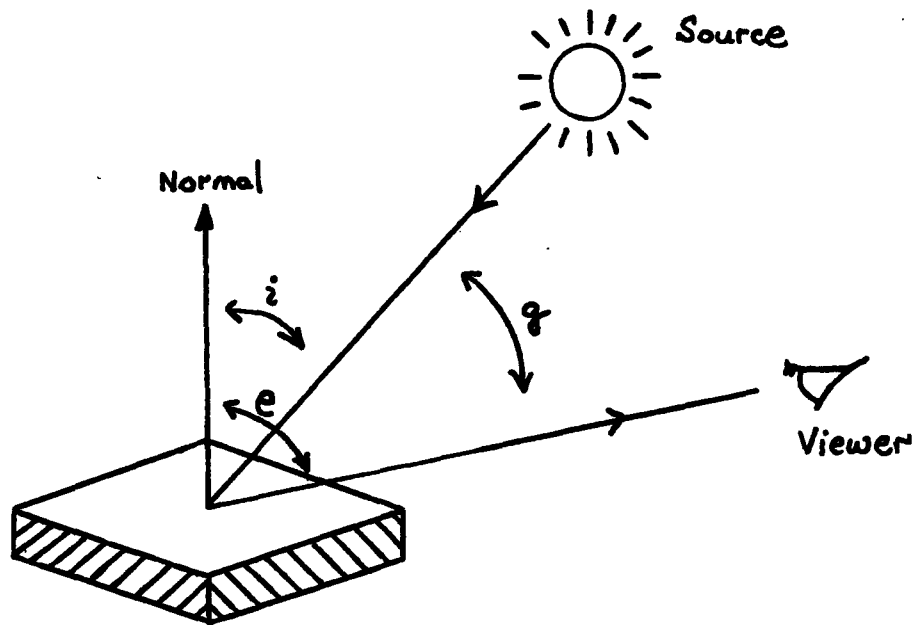
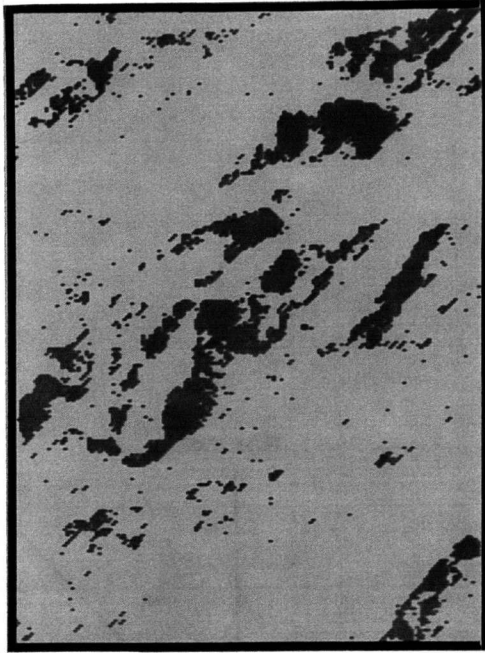
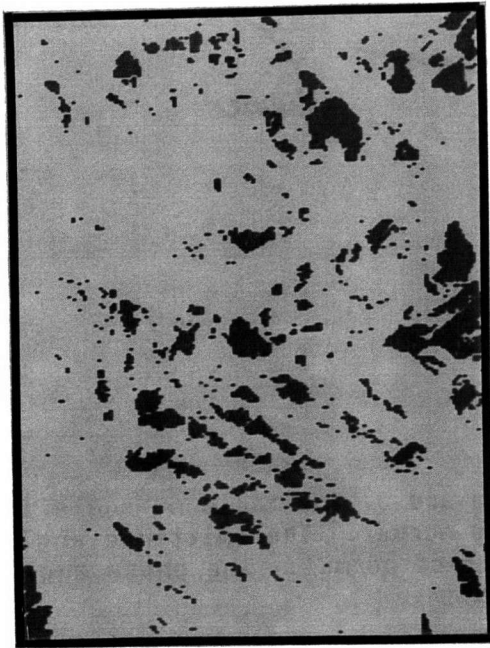


Figure 2 Defining the three photometric angles i , e and g . The incident angle i is the angle between the incident ray and the surface normal. The emittance angle e is the angle between the emergent ray and the surface normal. The phase angle g is the angle between the incident and emergent rays.



3 a)



3 b)

Figure 3 Shadow points. Figure 3(a) corresponds to early morning (9:55 GMT 1972/Oct/9). Figure 3(b) corresponds to early afternoon (13:48 GMT 1972/Oct/9).

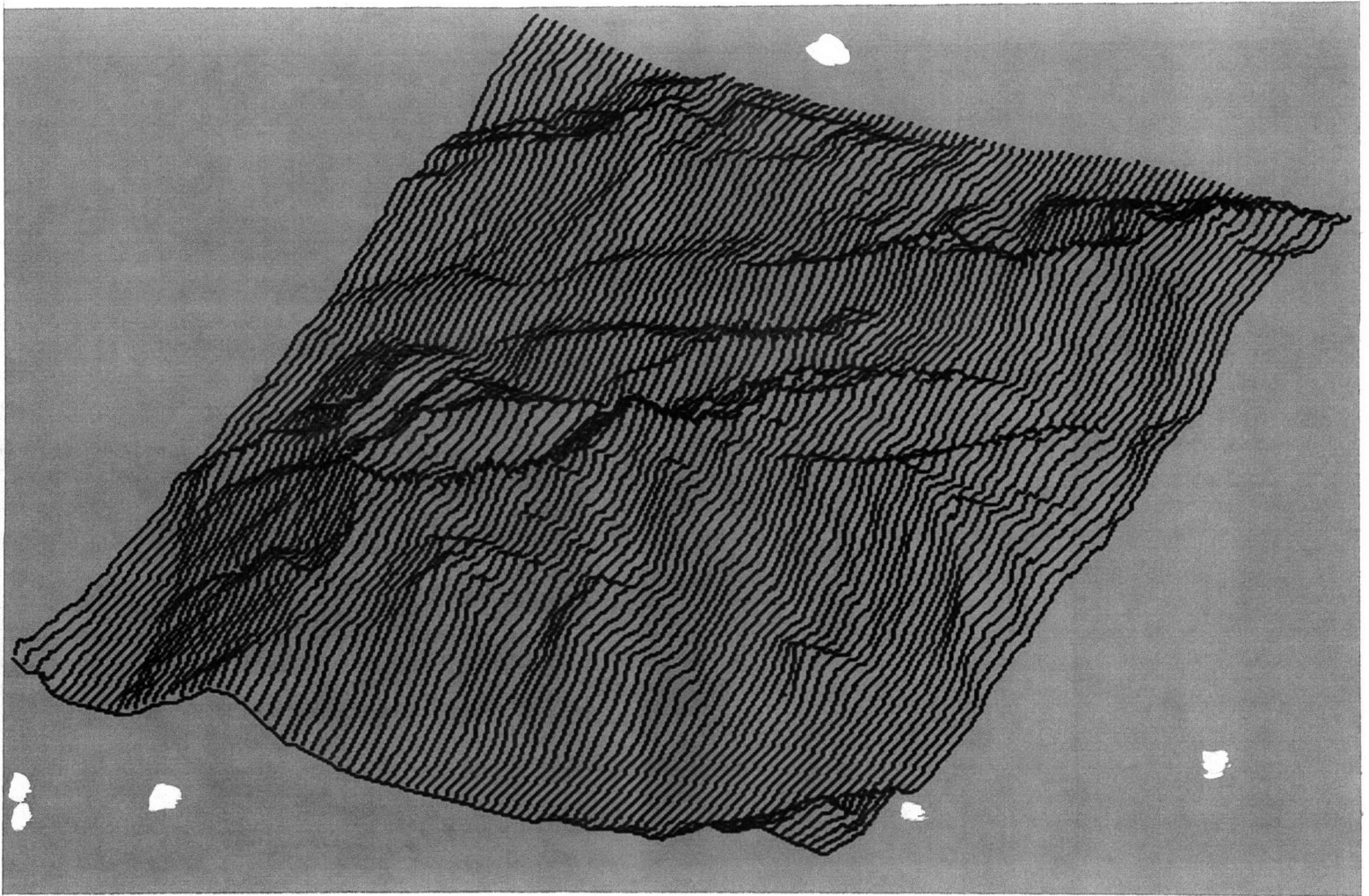


Figure 4 a) The terrain as seen from the sun in the early morning (9:55 GMT).

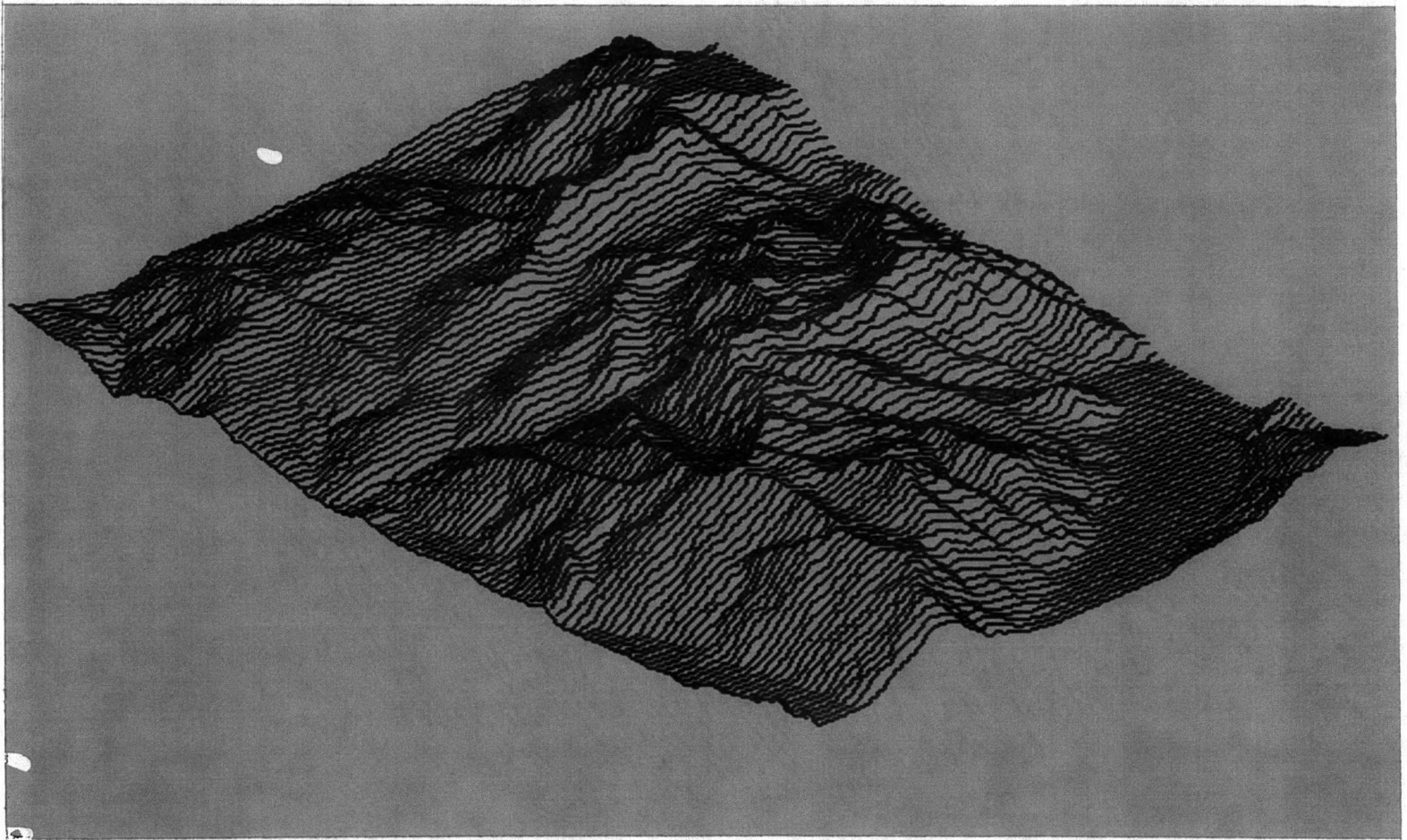


Figure 4 b) The terrain as seen from the sun in the early afternoon (13:48 GMT).

Figure 5 Plots of intensity versus terrain elevation for points lying in shadow. Figure 5(a) corresponds to band 4 (500-600 nm). Figure 5(b) corresponds to band 5 (600-700 nm). Figure 5(c) corresponds to band 6 (700-800 nm). Figure 5(d) corresponds to band 7 (800-1100 nm).

32

BAND 4



Image
Irradiance

0

410 m

Elevation

3210 m

5/22/78 14:17:46 30 BWOOD L BWOOD TTYI 1Z 0:02:58.8 16/191K

32

BAND 5



Image
Irradiance

0

410 m

Elevation

3210 m

5/22/78 14:20:05 30 BWOOD L BWOOD TTYI 12 0:03:05.7 47/191K

32

BAND 6



Image
Irradiance

0

410 m

Elevation

3210 m

5/22/78 14:22:25 30 BWOOD L BWOOD TTYI 32 0:03:13.6 137/191K

32

BAND 7

Image
Irradiance

0

410 m

Elevation

3210 m

5/22/78 14:24:17 30 BWOOD L BWOOD TTYI 3Z 0:03:21.5 125/191K